Communications

Novel Iridium Complexes Containing 2,6-Bis(oxazoline)pyridine Ligands: Synthesis and Reactivity of the Diolefin Iridium(I) Complex $[Ir(\eta^2\text{-}C_2H_4)_2\{\kappa^3N,N,N\text{-}(S,S)\text{-}i\text{-}Pr\text{-}pybox\}][PF_6]$ ((*S,S*)-*i*-Pr-pybox = 2,6-Bis(4′-(*S*)-isopropyloxazolin-2′-yl)pyridine)

Josefina Díez, M. Pilar Gamasa,* José Gimeno, and Paloma Paredes

Departamento de Química Orgánica e Inorgánica, Instituto de Química Organometálica "Enrique Moles" (Unidad Asociada al CSIC), Facultad de Química, Universidad de Oviedo, 33071 Oviedo, Spain

Received February 2, 2005

Summary: The novel iridium(I)-pybox complexes $[Ir(L)_n\{\kappa^3N,N,N\text{-}(S,S)\text{-}i\text{-}Pr\text{-}pybox\}][PF_6]$ *(n = 2, L =* η^2*-*C_2H_4 *(**1**),* η^2*-*$MeO_2CC{\equiv}CCO_2Me$ *(**2**); n = 1, L = CO (**3**)) have been synthesized. The treatment of complex **1** with HCl or allyl chloride under very mild conditions results in the stereoselective formation of the complexes* $[IrClH(\eta^2\text{-}C_2H_4)\{\kappa^3N,N,N\text{-}(S,S)\text{-}i\text{-}Pr\text{-}pybox\}][PF_6]$ *(**4**) and* $[IrCl(\eta^3\text{-}C_3H_5)\{\kappa^3N,N,N\text{-}(S,S)\text{-}i\text{-}Pr\text{-}pybox\}][PF_6]$ *(**5**). The structures of complexes **1** and **5** have been determined by X-ray diffraction analyses.*

Asymmetric catalysis with complexes containing enantiopure 2,6-bis(oxazoline)pyridine ligands (R-pybox; pybox = 2,6-bis(oxazolin-2′-yl)pyridine, R = *i*-Pr, Ph, Bn, etc.) has received considerable attention in the last 15 years. A recent and specific survey illustrates the state of the art of this field.[1] Despite the fact that extensive studies on the catalytic activity of these species in asymmetric carbon−carbon bond-forming reactions have been undertaken, most of the metal-pybox catalysts have been prepared in situ and only a few of them have been characterized. Among them, octahedral complexes of group 8 and 9 metals (d^6 ruthenium(II) and rhodium(III) complexes) are excellent catalysts for the enantioselective cyclopropanation of olefins ($[RuCl_2(\eta^2\text{-}C_2H_4)$(pybox)])[2] and hydrosilylation of ketones ($[RhCl_3$(pybox)]).[3] Recently we reported the first example of asymmetric transfer hydrogenation of ketones with chiral pybox complexes. Thus, *cis*- and *trans*-$[RuCl_2$(L)\{(*R,R*)-Ph-pybox\}] (L = phosphine, phosphite) complexes are active catalysts leading to the formation of *sec*-alcohols with high levels of conversion and enantioselectivity. Indeed, some of them behave as efficiently as the best catalysts previously reported (up to 94% ee).[4]

As far as we know, only two examples of asymmetric catalysis using $[IrCl(cod)]_2$/pybox mixtures as catalyst have been reported. Thus, $[IrCl(cod)]_2$/indane-pybox has been used recently by Morken and co-workers to catalyze a reductive aldol reaction.[5] They assume that initially the pybox ligand binds to metal in a three-coordinate fashion and then an iridium(I) hydride intermediate is formed via oxidative Si−H addition and reductive Si−Cl elimination. However, they were not able to crystalize any iridium-pybox complex. A regio- and enantioselective allylic substitution catalyzed by $[IrCl(cod)]_2$/Ph-pybox has also been reported last year.[6]

On the grounds of these recent results, we are interested in exploring the synthesis of iridium-pybox complexes as well as investigating subsequently their potential applications in asymmetric catalytic processes.

This communication describes the synthesis of the first iridium-pybox complexes, such as (a) the cationic diolefin $[Ir(\eta^2\text{-}C_2H_4)_2\{\kappa^3N,N,N\text{-}(S,S)\text{-}i\text{-}Pr\text{-}pybox\}][PF_6]$ (**1**), dialkyne $[Ir(\eta^2\text{-}MeO_2CC{\equiv}CCO_2Me)_2\{\kappa^3N,N,N\text{-}(S,S)\text{-}i\text{-}Pr\text{-}pybox\}][PF_6]$ (**2**), and monocarbonyl $[Ir(CO)\{(\kappa^3N,N,N\text{-}(S,S)\text{-}i\text{-}Pr\text{-}pybox\}][PF_6]$ (**3**) iridium(I) complexes and (b) hydride $[IrClH(\eta^2\text{-}C_2H_4)\{\kappa^3N,N,N\text{-}(S,S)\text{-}i\text{-}Pr\text{-}pybox\}][PF_6]$ (**4**) and η^3-allyl $[IrCl(\eta^3\text{-}C_3H_5)\{\kappa^3N,N,N\text{-}(S,S)\text{-}i\text{-}Pr\text{-}pybox\}][PF_6]$ (**5**) iridium(III) complexes.

The reaction of a suspension of $[IrCl(coe)_2]_2$ (coe = cyclooctene) in methanol with ethene (1 atm) at room temperature followed by addition of 2 equiv of *i*-Pr-pybox (*i*-Pr-pybox = 2,6-bis[4′-(*S*)-isopropyloxazolin-2′-yl]pyridine) at −40 °C, under an ethene atmosphere, affords, after anion exchange with $NaPF_6$ and workup, the complex $[Ir(\eta^2\text{-}C_2H_4)_2\{\kappa^3N,N,N\text{-}(S,S)\text{-}i\text{-}Pr\text{-}pybox\}][PF_6]$ (**1**) as an orange solid in excellent yield (94%).[7,8] In the absence of $NaPF_6$ the complex $[Ir(\eta^2\text{-}C_2H_4)_2\{\kappa^3N,N,N\text{-}(S,S)\text{-}i\text{-}Pr\text{-}pybox\}][Cl]$ was isolated in poor yield (Scheme 1). The spectroscopic NMR data for **1** are

(1) Desimoni, G.; Faita, G.; Quadrelli, P. *Chem. Rev*. **2003**, *103*, 3119.
(2) Nishiyama, H.; Itoh, Y.; Matsumoto, H.; Park, S.-B.; Itoh, K. *J. Am. Chem. Soc.* **1994**, *116*, 2223.
(3) Nishiyama, H.; Kondo, M.; Nakamura, T.; Itoh, K. *Organometallics* **1991**, *10*, 500.
(4) Cuervo, D.; Gamasa, M. P.; Gimeno, J. *Chem. Eur. J*. **2004**, *10*, 425.
(5) Zhao, C.-X.; Duffey, M. O.; Taylor, S. J.; Morken, J. P. *Org. Lett.* **2001**, *3*, 1829.
(6) Miyabe, H.; Matsumura, A.; Moriyama, K.; Takemoto, Y. *Org. Lett*. **2004**, *6*, 4631.

10.1021/om050073x CCC: $30.25
Publication on Web 03/16/2005

Scheme 1

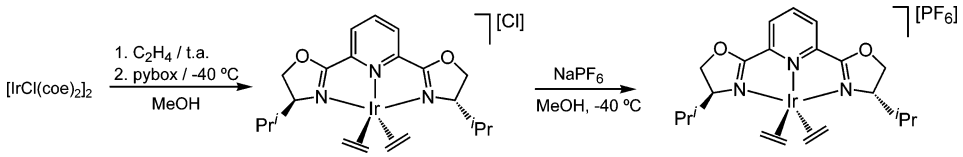

consistent with the presence of a C_2 symmetry axis. The most significant features in the ^{1}H and ^{13}C{^{1}H} NMR spectra are a broad singlet at 2.89 ppm and a singlet at 32.14 ppm, which are assigned to the hydrogen[9] and carbon atoms, respectively, of the ethylene ligands. These data are consistent with a fast rotation of the olefin ligands around their respective metal−ligand axes at room temperature on the NMR time scale.[10] Variable-temperature ^{1}H NMR studies (291−183 K) confirme the dynamic behavior of the olefin ligand in complex **1**. Thus, the broad singlet resonance observable in the spectrum at room temperature splits at low temperature (203 K) into four multiplets (3.80, 3.50, 2.04, and 1.89 ppm). The estimated activation barrier $\Delta G^{\ddagger}$ for ethene rotation[11] is 44.5 kJ/mol, a value that is rather low if it is compared with those usually observed for other olefin iridium(I) complexes.[12] The ^{13}C{^{1}H} NMR spectrum recorded at 203 K shows also two singlet signals (36.68 and 23.79 ppm) for the two olefin carbon atoms.

The structure of complex **1** has been determined by a single-crystal X-ray diffraction study.[13] The geometry around the iridium atom is intermediate between the square pyramid and the trigonal bipyramid idealized extremes, with iridium bonded to the tridentate pybox fragment and to the two η^2-bound molecules of ethene (Figure 1). Thus, the sterochemistry at iridium can be described as a distorted trigonal bipyramid in which the equatorial plane of the coordination polyhedron contains the pyridinic nitrogen and the midpoint of each ethene ligand, while the oxazoline nitrogen atoms are placed in apical positions. The equatorial plane defined by the N(2), the iridium atom, and the midpoint (CT01) of the C(1)−C(2) bond is almost perpendicular to the plane defined by N(1)−Ir−N(2) (dihedral angle 85.83°). The olefin carbon−carbon bond length, C(1)−C(2) (1.414(16) Å), is longer than for free ethene (1.339 Å),[14] as was found in other olefin iridium(I) complexes.[15] The N(1)−Ir−N(1b) angle (155.6°) is similar to that found in other six-coordinate octahedral pybox complexes.[16]

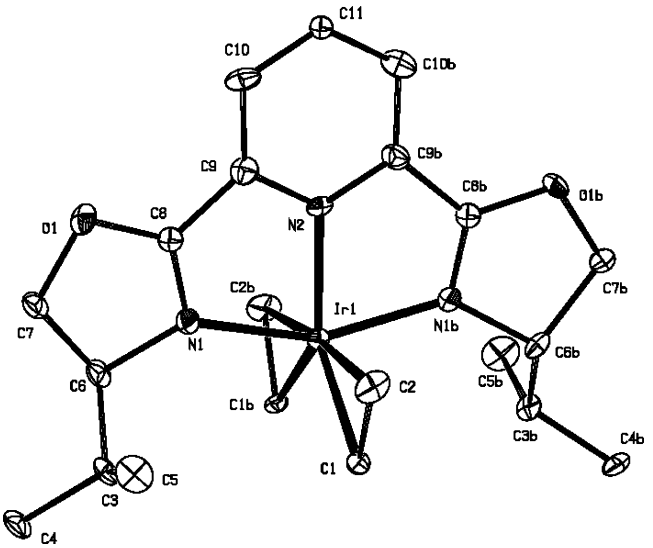

Figure 1. ORTEP drawing of the structure of [Ir(η^2-C_2H_4)$_2$(κ^3*N,N,N*-(*S,S*)-*i*-Pr-pybox)][PF_6] (**1**) showing the atom-labeling scheme. Atoms labeled with an "a" are related to those indicated by a crystallographic C_2 symmetry axis. Thermal ellipsoids are drawn at the 30% probability level. Hydrogen atoms and the PF_6^- anion are omitted for clarity. Selected bond lengths (Å) and angles (deg): Ir−N(1), 2.041(10); Ir−N(2), 2.015(10); Ir−C(1), 2.138(12); Ir−C(2), 2.104(14); C(1)−C(2), 1.414(16); Ir−CT01, 2.0089(1); N(2)−Ir−N(1), 77.8(3); N(2)−Ir−C(1), 132.3(3); N(2)−Ir−C(2), 93.4(4); N(2)−Ir−CT01, 113.01. CT01 = midpoint of C(1)−C(2) bond length.

The reaction of [Ir(η^2-C_2H_4)$_2${κ^3*N,N,N*-(*S,S*)-*i*-Pr-pybox}][PF_6] (**1**) with 2 equiv of dimethyl acetylenedicarboxylate in acetonitrile for 3 min results in the replacement of two ethylene ligands and the fast formation of the complex [Ir(η^2-$MeO_2CC{\equiv}CCO_2Me$)$_2${κ^3*N,N,N*-(*S,S*)-*i*-Pr-pybox}][PF_6] (**2**). By addition of diethyl ether

(7) A flow of ethylene was slowly bubbled at room temperature into a suspension of [IrCl(coe)$_2$]$_2$ (0.448 g, 0.5 mmol) in 5 mL of methanol. After the solution became yellow, *i*-Pr-pybox (0.301 g, 1 mmol) was added and the mixture stirred at −40 °C for 40 min. To the resulting red solution was added $NaPF_6$ (0.248 g, 1.45 mmol), and the mixture was stirred at −40 °C for 45 min. Diethyl ether was added (ca. 100 mL), and the resulting orange solid was washed with cold ether (3 × 5 mL) and then vacuum-dried.

(8) All of the new complexes have been characterized by IR, ^{1}H and ^{13}C NMR, mass spectrometry (FAB) (for **2**), and microanalyses (for **1** and **3**−**5**) (see the Supporting Information).

(9) A markedly broad resonance due to the accidental degeneration of the geminal protons of ethene ligands is observed in complex **1**.

(10) Dissolution of C_2H_4 does not alter the ^{1}H and ^{13}C{^{1}H} NMR spectra; hence, no intermolecular exchange of ethene seems to be taking place; see: Mann, B. E. In *Comprehensive Organometallic Chemistry*; Wilkinson, G., Stone, F. G. A., Abel, E. W., Eds.; Pergamon Press: Oxford, U.K., 1982; Vol. 3, pp 103−109.

(11) Values estimated from the coalescence temperature (233 K) using the Eyring equation, $\Delta G^{\ddagger} = 19.14[9.97T_c + \log(T_c/\delta\nu)]$ (J/mol): Günther, H. *NMR Spectroscopy*, 2nd ed.; Wiley: New York, 1995; p 343.

(12) Activation barriers, $\Delta G^{\ddagger}$. (a) For the complex [IrTp(η^2-C_2H_4)$_2$] (Tp = hydrotris(pyrazol-1-yl)borate) (54.34 kJ/mol): Tanke, R. S.; Crabtree, R. H. *Inorg. Chem*. **1989**, *28*, 3444. (b) For cyclopentadienyl and indenyl iridium(I) complexes: [Ir(η^5-C_nH_m)(η^2-C_2H_4)L] (C_nH_m = C_5H_5, L = CO, C_2H_4; C_nH_m = C_9H_7, L = CO, C_2H_4) (ca. 58−84 kJ/mol): Szajek, L. P.; Lawson, R. J.; Shapley, J. R. *Organometallics* **1991**, *10*, 357. (c) For [Ir(η^5-C_5H_4R)(η^2-C_2H_4)L] (R = COCOOEt, L = C_2H_4; R = COOMe, L = C_2F_4) (67 and 72 kJ/mol, respectively): Arthurs, M. A.; Bickerton, J.; Stobart, S. R.; Wang, J. *Organometallics* **1998**, *17*, 2743. (d) For [Ir(η^2-C_2H_4)$_2$(dppe)]$^+$ (ca. 37 kJ/mol): Albietz, P. J.; Cleary, B. P.; Paw, W.; Eisenberg, R. *Inorg. Chem*. **2002**, *41*, 2095.

(13) X-ray data for complex **1** ($C_{21}H_{31}F_6IrN_3O_2P$): M_w = 694.66, red crystals, orthorhombic ($P2_12_12$), a = 15.3775(7) Å, b = 8.4994(3) Å, c = 9.2423(5) Å, $F(000)$ = 680, V = 1207.96(10) Å^3, T = 150(2) K, Z = 2, D_c = 1.910 g cm^{-3}, μ(Cu Kα) = 11.971 mm^{-1}, R = 0.0431, R_w = 0.1139 (observed data with $I > 2\sigma(I)$), absolute structure parameter 0.01(3).

(14) Stoicheff, B. P. *Tetrahedron* **1962**, *17*, 135.

(15) (a) For the complex [IrTp*(η^2-C_2H_4)$_2$] (Tp* = hydrotris(3,5-dimethyl-1-pyrazol-1-yl)borate) (average 1.42(2) Å): Alvarado, Y.; Boutry, O.; Gutiérrez, E.; Monge, A.; Nicasio, M. C.; Poveda, M. L.; Pérez, P. J.; Ruíz, C.; Bianchini, C.; Carmona, E.; *Chem. Eur. J*. **1997**, *3*, 860. (b) For the complex [Ir(η^2-C_2H_4)$_2$(PMe_2Ph)$_3$][BF_4]·0.5H_2O (average 1.421(22) Å): Lundquist, E. G.; Folting, K.; Streib, W. E.; Huffman, J. C.; Eisenstein, O.; Caulton, K. G. *J. Am. Chem. Soc*. **1990**, *112*, 855.

(16) In rhodium(III) complexes. (a) [$RhCl_3$(κ^3*N,N,N*-*i*-Pr-pybox)] (158.7°): see ref 3. (b) [Rh(CH_3)I(κ^3*N,N,N*-*i*-Pr-pybox)(CO)][PF_6] (156.5-(2)°): Cuervo, D.; Díez, J.; Gamasa, M. P.; García-Granda, S.; Gimeno, J. *Inorg. Chem*. **2002**, *41*, 4999. In ruthenium(II) complexes. (c) *cis*-[$RuCl_2$(PPh_3)(κ^3*N,N,N*-*i*-Pr-pybox)] (155.8(3)°): Cadierno, V.; Gamasa, M. P.; Gimeno, J.; Iglesias, L.; García-Granda, S. *Inorg. Chem*. **1999**, *38*, 2874.

Scheme 2

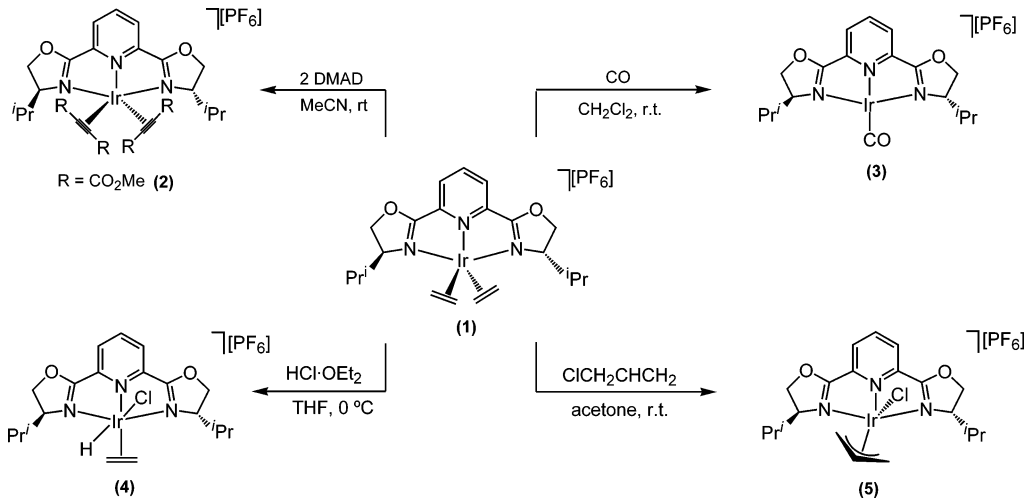

and hexane the complex **2** was isolated as an air-stable orange solid (86% yield) (Scheme 2). Furthermore, when 1 equiv of alkyne is used, the monosubstituted product is not formed, but the complex **2** along with small amounts of two unidentified complexes is obtained. The C_2 symmetry of the precursor **1** is still present in compound **2**, as indicated by the NMR data of **2**. Characteristic $^{13}C\{^1H\}$ NMR resonances for the MeO_2-CC≡CCO_2Me group are the singlets at 53.32 and 52.97 ppm (Me), 84.89 and 75.63 ppm (C≡C), and 161.99 and 157.08 ppm (CO), indicating no rotation of alkyne groups in solution at room temperature.

Complex **1** reacts also with carbon monoxide (1 atm) in dichloromethane. The IR spectrum in the ν(CO) region shows the initial formation of a dicarbonyl complex (ν(CO) 2088, 2021 cm^{-1}), which leads to the 16-electron monocarbonyl complex [Ir(CO){κ^3*N,N,N*-(*S,S*)-*i*-Pr-pybox}][PF_6] (**3**) (ν(CO) 1989 cm^{-1}) when the reaction mixture is worked up[17] (Scheme 2). Complex **3** is isolated as an air-stable yellow solid in excellent yield (96%). The NMR data are consistent with the C_2 symmetry structure, and a low-field singlet, δ 182.28 in the $^{13}C\{^1H\}$ NMR spectrum, confirms the presence of the carbonyl group.

Since oxidative additions are among the most usual steps that are proposed in catalytic cycles, we have investigated the stability of the diolefin complex **1** in this type of reaction. We are particularly interested in the synthesis of hydride and allyl complexes, types of species that are extensively found as intermediates in both stoichiometric and catalytic processes. The treatment of a solution of complex **1** in THF with a solution of HCl in diethyl ether at 0 °C followed by workup of the reaction mixture as described above for complex **2** leads to the complex [IrClH(η^2-C_2H_4){κ^3*N,N,N*-(*S,S*)-*i*-Pr-pybox}][PF_6] (**4**), isolated as a yellow solid in 94% yield (Scheme 2). The presence of the hydride is confirmed by ^1H NMR (δ −22.56 ppm) and IR (ν(Ir−H) 2186 cm^{-1}, medium intensity). The ^1H and $^{13}C\{^1H\}$ NMR spectra show the expected resonances for the ethylene group (a broad singlet at 4.77 ppm and a singlet at 59.99 ppm, respectively). The NMR and IR spectroscopic data are consistent with three possible stereoisomers. All attempts to crystallize **4** in a number of solvents were unsuccessful, and an X-ray analysis could not be performed. Further studies to chemically establish the full structure of **4** are in progress.

Next, the oxidative addition of allyl chloride to **1** has been explored. The reaction of complex **1** with allyl chloride (1:1.5 molar ratio) in acetone at room temperature results in the fast formation of a dark red solution from which the complex [IrCl(η^3-C_3H_5){κ^3*N,N,N*-(*S,S*)-*i*-Pr-pybox}][PF_6] (**5**) is isolated as an orange solid in 93% yield[18] (Scheme 2). The expected olefin complex intermediate with a monodentate allyl group is not detected. The ^1H NMR spectrum of complex **5** shows four doublets for the syn (δ 4.92 and 3.52, J_{HH} = 6.9

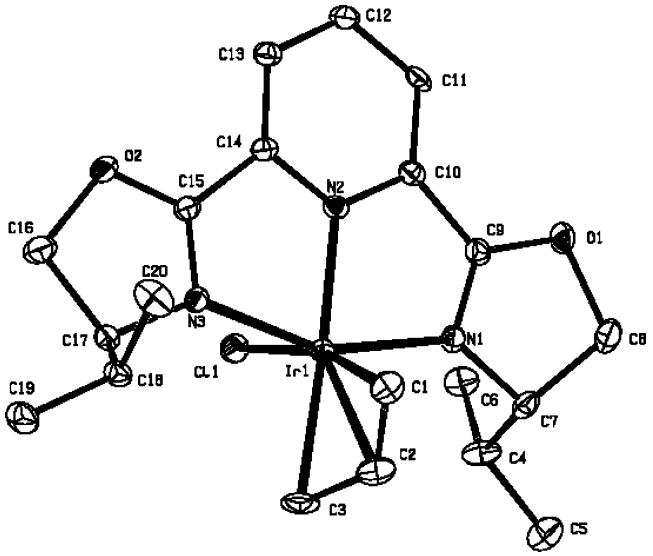

Figure 2. ORTEP drawing of the structure of [IrCl(η^3-C_3H_5)(κ^3*N,N,N*-(*S,S*)-*i*-Pr-pybox)][PF_6] (**5**) showing the atom-labeling scheme. Thermal ellipsoids are drawn at the 10% probability level. Hydrogen atoms and the PF_6^- anion are omitted for clarity. Selected bond lengths (Å) and angles (deg): Ir−N(1), 2.063(6); Ir−N(2), 2.018(5); Ir−N(3), 2.071(5); Ir−Cl(1), 2.4223(18); Ir−C(1), 2.139(7); Ir−C(2), 2.119(8); Ir−C(3), 2.207(8); C(1)−C(2), 1.42(2); C(2)−C(3), 1.282(15); N(2)−Ir−N(1), 77.5(2); N(2)−Ir−N(3), 78.1(2); N(1)−Ir−N(3), 155.6(2); Cl(1)−Ir−C(1), 165.9(4); N(2)−Ir−C(3), 173.5(3); N(3)−Ir−C(1), 94.5(4); N(1)−Ir−C(1), 93.1(3).

(17) After CO bubbling, the resulting solution was concentrated and diethyl ether was added to yield **3** as a dark green solid. Complex **3** was obtained in higher purity if a flow of nitrogen was slowly bubbled into the dichloromethane solution over 50 min and then worked up as above.

Hz) and anti hydrogen atoms (δ 3.95 and 2.76, J_{HH} = 11.7 Hz) of the η^3-allyl ligand as well as a multiplet at 5.60 ppm for the central allyl hydrogen. The allyl group is observed in the $^{13}C\{^1H\}$ NMR spectrum as three singlets at 95.77 ppm (C-2) and 44.19 and 27.04 ppm (C-1 and C-3). The spectra are in accordance with a rigid structure of the allyl group in solution at room temperature.

The X-ray crystal structure determination of complex **5**[19] shows a pseudooctahedral geometry around the iridium atom, which is bonded to the chloride atom and to the three nitrogen atoms of the pybox ligand, the η^3-allyl fragment formally occupying two coordination sites (Figure 2). Concerning the bond lengths within the allyl moiety, the shorter bond distance of C(2)−C(3) (1.282(15) Å) with respect to C(1)−C(2) (1.42(2) Å) is remarkable, a fact that reveals the allyl ligand to be highly unsymmetrical and distorted toward a σ-π^2-type coordination.[20] Similar distortions have been found in other allyl complexes of iridium.[20,21] As is characteristic for η^3-allyl complexes, the iridium−carbon central bond distance (Ir−C(2) = 2.119(8) Å) is shorter than Ir−C(3) (2.207(8) Å) and Ir−C(1) (2.139(7) Å). The longer Ir−C(3) distance is probably due to the higher trans influence of the pyridine nitrogen with respect to the chloride atom. On the other hand, the three N−Ir−N bond angles (77.5(2), 78,1(2), and 155.6(2)°) fall in the range observed for complex **1** and are analogous to those encountered in other κ^3-pybox species.[16]

In summary, this paper has dealt with the synthesis of organoiridium(I) and -iridium(III) complexes containing enantiopure pybox ligands. Interestingly, these types of iridium complexes have not been hitherto reported and, in addition, they are potentially useful in asymmetric catalytic processes. Further studies concerning their reactivity in stoichiometric and catalytic processes are in progress.

Acknowledgment. This work was supported by the Ministerio de Ciencia y Tecnología (MCT) (BQU2003-00255) and FICYT (project PR-01-GE-4). P.P. thanks the Ministerio de Educación y Cultura (MEC) of Spain for the award of a Ph.D. grant.

Supporting Information Available: Text and tables giving complete details of the experimental procedures and spectroscopic data (IR and ^1H and ^{13}C NMR) for new compounds and crystallographic data for **1** and **5**; crystallographic data are also given as CIF files. This material is available free of charge via the Internet at http://pubs.acs.org.

OM050073X

(18) Allyl chloride (0.026 mL, 0.3 mmol) was added to a solution of the complex **1** (0.138 g, 0.2 mmol) in 10 mL of acetone. The solution was stirred at room temperature for 5 min, the volatiles were removed under vacuum, and the deep red residue was extracted with CH_2Cl_2. Hexane was added, and the solution was concentrated and cooled to −20 °C, giving an orange microcrystalline solid, which was washed with hexane (3 × 5 mL) and vacuum-dried.

(19) X-ray data for complex **5**: ($C_{20}H_{28}ClF_6IrN_3O_2P$), M_w = 715.07, orange crystals, monoclinic ($P2_1$), a = 8.2524(5) Å, b = 16.0006(10) Å, c = 9.4409(6) Å, β = 91.441(5)°, $F(000)$ = 696, V = 1246.21(13) Å^3, T = 293(2) K, Z = 2, D_c = 1.906 g cm^{-3}, μ(Cu Kα) = 12.590 mm^{-1}, R = 0.0311, R_w = 0.0698 (observed data with $I > 2\sigma(I)$), absolute structure parameter −0.015(12).

(20) Fryzuk, M. D.; Gao, X.; Rettig, S. J. *J. Am. Chem. Soc.* **1995**, *117*, 3106.

(21) Bartels, B.; García-Yebra, C.; Rominger, F.; Helmchen, G. *Eur. J. Inorg. Chem.* **2002**, 2569.